AIMS Materials Science, 8(4): 538–549.
DOI: 10.3934/matersci.2021033
Received: 04 March 2021
Accepted: 20 June 2021
Published: 30 June 2021

http://www.aimspress.com/journal/Materials

Research article

Physical analysis and production—mechanics of glass-ceramic prototypes made by sintering cold-compacted powder samples (10% slag, 70% fly ash and 20% glass cullet)

Diana. M. Ayala Valderrama[1,*], Jairo A. Gómez Cuaspud[2] and Leonel Paredes-Madrid[3]

[1] Comprehensive Management of Agro-industrial Productivity and Services GISPA, Santo Tomas University, Tunja, Av. Universitaria, No. 45-202. Tunja, Boyacá, Colombia
[2] Institute for Research and Innovation in Materials Science and Technology, Pedagogical and Technological University of Colombia, Av. Central del Norte, 39-115, Tunja, Boyacá, Colombia
[3] Faculty of Mechanic, Electronic and Biomedical Engineering, Universidad Antonio Nariño, Tunja 150001, Colombia

* **Correspondence:** Email: diana.ayala01@uptc.edu.co, diana.ayala@usantoto.edu.co;
Tel: +5732080955886.

Abstract: We carried out physicochemical and mechanical characterization studies of glass-ceramic materials obtained from industrial waste of slag, fly ash and glass cullet. These studies were performed through the sintering process of powder by means of cold compaction, in concentrations of 10% slag, 70% fly ash and 20% glass cullet. A total of 230 pellets of 15 mm diameter by 5 mm thickness were produced. Later, 15 pellets were heat treated with a heating ramp of 10 ºC/min up to 1000 ºC and held for 2 hours, followed by a cooling rate of 10 ºC/min. The remaining 15 pellets were heat treated with a heating ramp of 10 ºC/min up to 1050 ºC, followed by the same hold and cooling times. The increase in temperature favored the mechanical resistance of the glass-ceramic and the phases formed after the thermal treatments were anorthite, augite, gehlenite, and cordierite. The highest porosity found in this process was 40%; in terms of bulk densities, these were 2.36 and 2.57 g/cm^3. In contrast to the observations of mechanical resistance, crystalline phases, apparent porosity, bulk density and chemical resistance. They showed that the temperature increase decreased the percentage of porosity and increased the values of densities and mechanical properties. Scanning electron microscopy images using backscattered electrons confirmed the homogenization of the mixtures in both heat treatments and mechanical properties similar to those reported for glass-ceramic materials for construction industry applications.

Keywords: glass-ceramic; slag; glass cullet; fly ash; cold compaction

1. Introduction

The use of natural resources as raw materials in production processes is currently being evaluated for the negative impact on the environment associated with the depletion of energy resources and environmental degradation aspects that are not sustainable. This is one of the reasons why this research was focused on reincorporating into the production cycles those solid wastes that are generated in industrial processes, such as in the generation of electrical energy, in the production of steel, and in the production and post-use of glass. Therefore, we evaluated the possibility of extracting vitro-ceramic material from the combined use of 10% slag, 70% carbon fly ash and 20% glass cullet, sintering the powder samples by cold compaction and obtaining vitro-ceramic materials with applications mainly for the construction industry thanks to their good mechanical and chemical properties, and their high resistance to thermal shock.

Glass ceramics have drawn interest in different application fields, such as ceramic components, high-tech materials, building materials, composite materials, and thermal shock resistant materials, such as kiln refractories. Furthermore, they are becoming promising materials thanks to the possibility of being manufactured with different types of industrial waste as a source of aluminosilicate components. Therefore, glass-ceramic technology allows industrial waste materials that are currently sent to landfill to become useful products for society [1–6].

We researched the influence of the powder sintering procedure by cold compaction for the production of glass-ceramic samples, as well as the influence that heat treatment has on strength and microstructure. We identified the crystalline phases by means of XRD analysis, and we carried out chemical resistance analysis, thermal shock resistance evaluating the microstructure and its changes in mechanical resistances, and finally we calculated the density and apparent porosity of the obtained materials following the methodology defined in the ASTM C20-00 and ASTM C373 standards. The forming process by sintering of cold compacted powder samples is one of four methods carried out by Rawling [3]. It consists of taking samples in powder form that are cold compacted into tablets of different dimensions, followed by a heat treatment at high temperatures for sintering, achieving the nucleation and crystallization of the material in a single thermal process. The material sintered by this process comprised two temperatures (1000 and 1050 ºC) for 2 hours. These thermal treatments were carried out in order to obtain a material with an amorphous structure and crystalline phases, among which the phases of diopsite, anorthite, gehlenite, augite and enstatite stand out; they have good mechanical properties, chemical resistance and thermal shock resistance. In a general way, this work shows the results of a study which objective was focused on showing the benefits of slag, fly ash, glass cullet as a raw material in obtaining glass-ceramic materials with adequate properties to be used as construction materials.

Low sintering temperatures were chosen for this study for the following reasons: (1) multiple studies have considered high sintering temperatures and time [7–9], therefore an innovative aspect of this research is to evaluate the resulting material obtained from sintering temperatures around 1000 ℃, (2) lower sintering temperatures yield lower cost of material production at industrial scale.

This work was carried out in collaboration with the Friedrich–Alexander University Erlangen–Nürenberg, Institute for Biomaterials, Department of Engineering and Materials Science.

2. Materials and methods

For the development of this study, the following raw materials were used: Fly ash obtained from different thermoelectric power plants whit classification as Class F according to ASTM C 618 standards, and iron oxide (ESC2) rich slag provided by steel industries located in the Department of Boyac á (Colombia). These two raw materials have an average particle size of 75 μm. We also used sodium-calcium glass cullet from the collection of household waste converted into fine powders with a particle size of <149 μm. The chemical composition of the raw materials was determined by XRF analysis as shown in Figure 1.

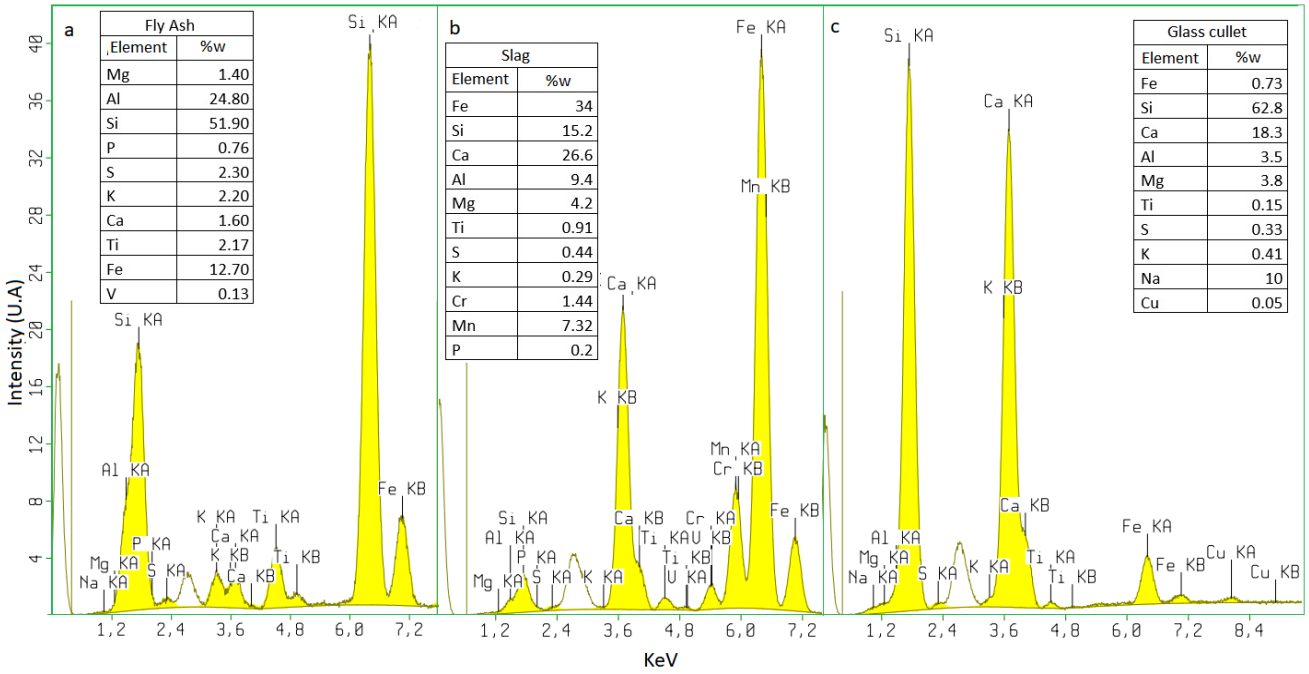

Figure 1. XRF X-ray fluorescence analysis of precursor materials associated with: (a) fly ash, (b) slag, (c) glass cullet.

2.1. Method for the preparation of glass-ceramic material by sintering of cold-compacted powder samples

This procedure comprised the uniaxial cold pressing of powders. This activity was performed to the material by applying pressure in one single direction until the total compaction of the powders was achieved using a hydraulic press at 30 MPa. Two different heat treatments were applied to the 30 assembled pellets, 15 pellets were heat treated with a heating ramp of 10 ºC/min up to 1000 ºC and held for 2 hours, followed by a cooling rate of 10 ºC/min. The remaining 15 pellets were heat treated with a heating ramp of 10 ºC/min up to 1050 ºC, followed by the same hold and cooling times. The whole process let us obtain viscosity flow as a diffusion mechanism that is related to the directed transport of a relatively low number of vacancies.

The sintering temperatures of 1000 and 1050 ℃ were chosen based on DTA analysis reported in authors' previous work [10].

2.2. Characterization techniques

The microstructural analysis of the morphological evaluation and surface characterization of the materials was performed by scanning electron microscopy (SEM) equipped with an energy dispersive X-ray spectroscopy (SEM-EDX) (LEO 435 Electron Microscope Ltd, Cambridge, UK and Ultra Plus, Zeiss, Jena, Germany). The structural analysis was performed by X-ray diffraction (XRD) on powder samples in a Bruker D8 Advance diffractometer (Karlsruhe, Germany) using CuKα radiation (1.5418 Å) with 2Θ in the range of 10–50 ° and a step size of 0.020 °. Crystal phase formation was corroborated using the Match program supported by the PDF-2 database (ICDD, International Centre for Diffraction Data, Newtown Square, PA).

The thermal shock resistance behavior of glass-ceramic materials was studied by measuring the compression resistance using the Zwick Roell (Ulm, Germany, series Z050) and microstructure (LEO 435, LEO Electron Microscopy Ltd., Cambridge, United Kingdom, and Ultra Plus, Zeiss, Jena, Germany). The thermal shock test was performed following the procedure set forth in "ASTM C1525-18, Standard Test Method for Determination of Resistance to Thermal Shock for Advanced Ceramics by Rapid Water Cooling". Samples of each sintered material were placed in an oven at 200, 500 and 800 ºC for a 10-minute holding period followed by rapid cooling to room temperature (22 ºC). The incidence of thermal shocks on the mechanical strength of the materials was evaluated by means of a compression test performed on granules of ~14 mm diameter with ~2.5mm thickness, using a universal testing machine (Zwick Roell, Ulm, Erlangen–Germany, Z050 Series) at a crossing speed of 0.5 mm/min, with a load cell of 30 kN. For each lot, a minimum of 5 samples were analyzed to evaluate the resistance of the materials.

Chemical analyses were carried out in acid medium, using 5 samples which were immersed in a 5% HCl solution for 24 hours with a drying process at 130 ºC/4 h, weighing and determining the percentage of mass loss. An analytical balance in triplicate with a measurement error of ± 0.0001 g was used.

Density and porosity were measured experimentally following the methodology described by ASTM C373 and ASTM C20 standards. The glass-ceramic granules were obtained by the method of cold compaction of powders. The preparation procedure involved compression at room temperature followed by drying at 150 ºC. After cooling, the granules were weighed using an analytical balance (MODEL Kern ABS 220 4N) with a tolerance of 0.01 g. This made it possible to determine the weight of the dry mass (D). Later, the granules were immersed in distilled water at boiling temperature for 5 hours, followed by 24 hours of soaking.

Immediately afterwards, the granules were weighed again; this allowed us to evaluate the suspended weight (S). The granules were then dried using a cotton towel to remove excess water from the surface. The granules were weighed to determine the saturated mass (W) [11,12]. With this data, we could determine the external volume (V) in cm^3 by subtracting the saturated mass from the suspended mass as follows (Eq 1):

$$V = (W-S)/\rho_w \quad (1)$$

where ρ_w stands for water density. The open porosity volume (OPV) can be determined from the difference between the saturated mass and the dry mass as follows (Eq 2).

$$OPV = W-D \quad (2)$$

As regards apparent porosity (P), it was calculated as a percentage from the open porosity data and volume as follows (Eq 3).

$$P = (OPV/V)*100\% \quad (3)$$

The bulk density (B) was determined from the dry mass ratio, D, and the external volume, V, including the pores as follows (Eq 4).

$$B = D/V \quad (4)$$

The units of bulk density are g/cm^3. Water absorption (A) is also an important metric of glass-ceramic materials. Water absorption can be expressed as a percentage of the volume ratio of open porosity and dry mass as follows (Eq 5).

$$A = (OPV/D)*100\% \quad (5)$$

3. Results and discussion

3.1. Processing of raw materials

First of all, it must be recalled that the sintering process occurred in two states; this condition was taken into account in order to determine the self-diffusion coefficient of crystals and the viscosity of solid fluids. The first sintering process occurred when the dust particles combined; during that time, an increment in the contact among particles and surface was observed. The second sintering process occurred during pore saturation, which is related with the diminishing of pores through diffusion along the material. Pores are defined as the countless concentration of defects and holes [13].

When using micro particles as raw material, the processing can be encompassed with the cluster model [14], The cluster model predicts smaller particles agglomeration occurring in the free spaced left behind by larger particles; thus inducing fast sintering in small particles. According to Scherer [15], each particle in sintering process has contact with 2 up to 6 neighboring particles, i.e. with borders and corners of structural unit. For the sake of our research that is related with real compacts, some particle may not have direct contact despite being relatively close to each other; this occurs when empty spaces appear among neighboring particles, which is known in literature as "frustrated contact". In other cases, the lack of neighboring particles creates a "hole" in the ordered structure. These types of defects reduce the densification speed of the structure.

According to the clusters model [14] in simultaneous crystallization, the solid impurities and the preexisting crystals in vitreous particles facilitate particle interactions that ultimately cause viscous flow. When this procedure takes place, it must be highlighted that additional effects may occur on sintering kinematics, such as: a reduction in densification rate due to either crystallization, or an increment in densification caused by the existence of sharp edges or by particles with a large aspect ratio, such as: the reduction in the rate of densification due to crystallization or there could also be an increase in densification due to the presence of sharp edges or particles that have various shapes (for example, powders with pointed shapes, in this case , the waste glass which is a starting material) Figure 2 shows an overview of the experimental scheme for the sintering of cold-pressed powder samples which were later used for the obtaining glass ceramic materials. The densification results of the pellets are shown in Section 3.5

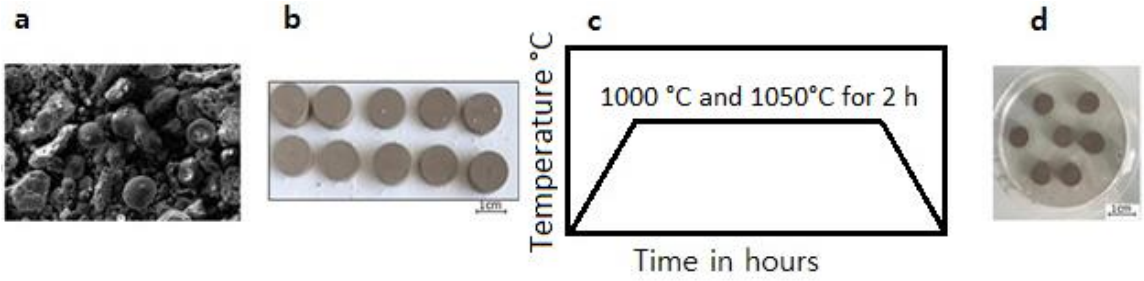

Figure 2**.** General diagram for the production of glass-ceramic material by the sintering method of cold compacted powder samples. (a) SEM image of mixture, (b) compacted mixture before heat treatment, (c) temperature diagram, and (d) pellets after heat treatment and cooling.

3.2. Microstructure

We got different microstructures of the glass-ceramic materials obtained by sintering cold-compacted powder samples. Structural morphologies were observed by scanning electron microscopy (SEM). The morphology of the grains with respect to the different thermal treatments in the material (10% ESC, 70% CeV, 20% CaV) are shown in Figure 3, where it can be seen that the morphology is not very well defined, forming a heterogeneous plate in all its extension. The presence of open porosity and grains with different morphology is clear, and we can also highlight the existence of a higher concentration of phases with spherical morphology, being probably the result of the presence of SiO_2 [16]. Specifically, in Figure 3a, a partial connection between particles is observed, identifying unreacted cenospheres, when the temperature increases by 50 ºC, i.e., working at 1050 ºC for 2 h (Figure 3b). We observed greater homogenization between particles, generating less porosity, improving the microstructure of the material. This morphology could affect the mechanical resistance of the material, because of the total non-compaction of the particles.

As can be seen from Figure 3a,b, a temperature change from 1000 up to 1050 ºC caused a noticeable increment in particles' sizes. It must be also noted that, the sintering of the fine particles caused the densification of the glass-ceramics at 1000 and 1050 ºC, and resulted in the increase of the compressive strength, as later described in Section 3.6

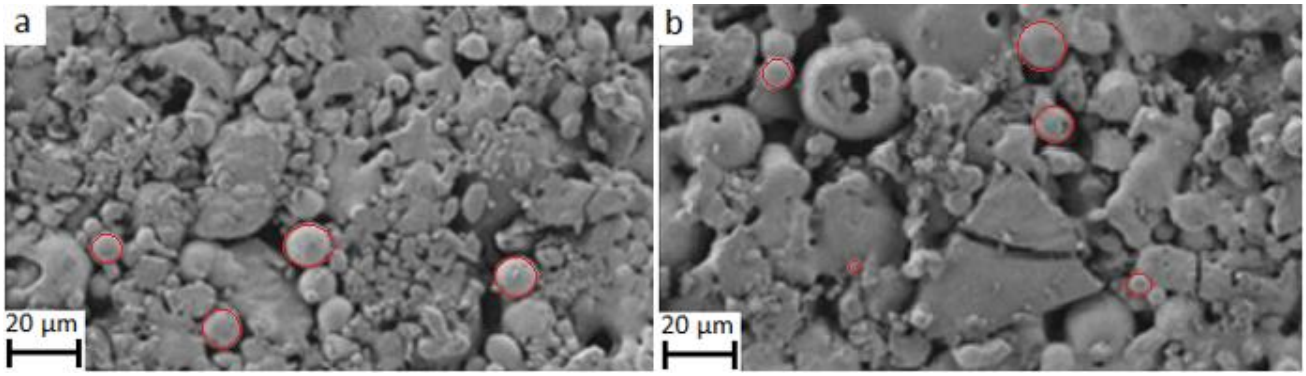

Figure 3. Scanning electron microscopy of heat treated material, (a) 1000 ºC for 2 h, (b) 1050 ºC for 2 h.

Spherical and sharp-angled particles can be distinguished and they could be identified as undissolved fly ash and unreacted glass. These particles appear well distributed in the amorphous glass-ceramic matrix. A large number of unreacted particles remained encapsulated at the surface in those samples that were treated at higher temperatures; however, in the microstructural observation in the materials obtained by sintering glassy powders, the crystallization volume increases when the temperature increases [17]. These materials exhibited good homogeneity and a reduced amount of unreacted particles with low porosity. In all sintered samples, long visible cracks and unreacted glass pieces are included. These defects within the microstructure reasonably caused the decrease of the mechanical resistance in the obtained materials.

3.3. X-Ray diffraction (XRD) analysis

Crystalline phases were identified by Rietveld refinement using the Match program supported by the PDF-2 database (ICDD, International Centre for Diffraction Data, Newtown Square, PA), where phase formation was evidenced, with their respective chemical composition and PDF number as follows: anorthite ($O_{64}Ca_8Si_{16}Al_{16}$ #PDF 96-100-0035), augite ($Na_{0.36}Ca_{2.46}Mg_{3.61}Fe_{0.84}Al_{1.37}Ti_{0.08}Si_{7.28}O_{24}$ #PDF 96-100-0036), gehlenite ($Ca_4Al_4Si_2O_{14,}$ #PDF 96-100-0049) and cordierite ($Si_{20.12}Al_{15.88}Mg_{7.64}Fe_{0.32}Mn_{0.04}Na_{0.20}K_{0.08}Ca_{0.08}H_{4.48}O_{74.24}$ #PDF 96-900-0546). They were generated from solid-state reactions in the sintering process, an aspect corroborated by X-ray diffraction (XRD) analysis. In general, the results revealed the formation of 4 phases (described in Figure 4) with variations in the percentages of phase contents in each sintered material [18].

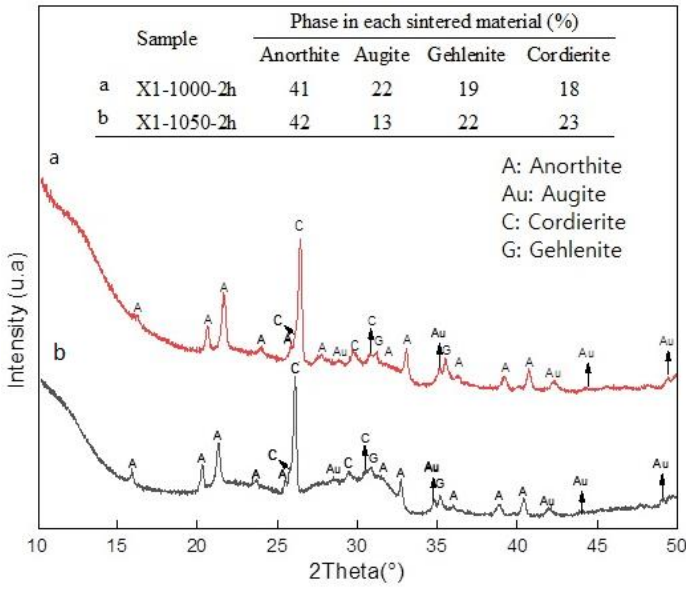

Figure 4. X-ray diffraction patterns and crystalline phases identified in the glass-ceramic materials, obtained by sintering cold-compacted powder samples.

The analysis of the relative weights in the inset table of Figure 4 showed that the anorthite phase is the main phase with 41% content when the material was sintered at 1000 ºC. As the temperature

increased, there was a small increase in variation in the percentage of this phase. Usually the anorthite phase develops in materials with a higher percentage of SiO_2 concentration and is a common phase in glass-ceramic materials that contributes to their mechanical strength. Augite is the second phase identified in the material, which due to its structure gives glass-ceramic materials good mechanical properties related to resistance to bending and good hardness [19,20]. The material showed 22% of the augite phase when sintered at 1000 ºC for 2 hours, which decreased as the sintering temperature was increased to 1050 ºC, obtaining 13% by weight of this phase. This aspect could be related to the crystallization process of the fly ash and slag, in addition to the Fe^{3+} content, which would be acting as a modifier of the glass structure in the process of breaking the Si-O-Si bonds, thus forming the augite phase [17,21].

Regarding the gehlenite phase, it increased when the temperature rose, achieving 19% phase content when sintered at 1000 ºC for 2 hours and 32% when sintered at 1050 ºC for the same time. It is important to note that the gehlenite phase is the only phase expected to form for low SiO_2 occupations [22]. It has been suggested that low temperature manufacturing and the existence of impurities, such as Na and K, reduce the stability of the crystalline structure of the gehlenite phase [23]. This phase occurs due to the reaction that takes place between the silica and the calcium oxide released in the calcite decomposition, which is favored by the conditions of homogeneity and permanence time during the experimental heating. However, there are no substantial differences with heating at 1000 and 1050 ºC in the relative proportions of the phases present [22]. It is suggested that the gehlenite phase was formed by the transformation of the merwinite phase treated at temperatures close to 1000 ºC. This phase was identified in the slag raw material object of this research and containing the sintered mixture; we observed the applicability to the devitrification of glass-ceramic materials with slag contents in their starting materials.

On the other hand, the percentage of the cordierite phase increased as the temperature rose, obtaining 18% at 1000ºC and 23% at 1050ºC for 2 hours. Crystalline phase interesting for electronic packaging materials, and presented in glass-ceramic materials for its majority content of Si and Al oxides, and traces of Mg, Fe, Mn, Na, K and Ca oxides [24]. Aspects that evidence the formation of crystalline phases from the sintering by cold compaction of industrial wastes of ESC, CaV and CeV evidencing the possibility of forming crystalline matrices ideal for the immobilization of wastes in the production of glass-ceramic materials [17].

3.3.1. Quantification of non-crystalline phase based on DRX

The quantification of non-crystalline and amorphous phases was done on the basis of X-ray diffractograms, which is a common method followed in specialized literature [25]. In our study, the software Origin was used for this purpose as follows: the area under the X-ray diffractogram was computed, but the zones associated with material crystallization were excluded. This procedure was applied for computing the amorphousness percentages of the two prototypes of glass ceramic materials; these materials were obtained on the basis of sintering cold-pressed powder samples. A 43% amorphous phase was measured for the prototype X1-1000-2h and 47% for the X1-1050-2h. It must be recalled that the transparency and impact resistance of glass ceramic materials is enhanced by the presence of amorphous zones. On the other hand, the occurrence of amorphous zones improves the tensile strength properties.

3.4. Chemical resistance of the produced glass-ceramic samples

In these chemical resistance experiments, 5 compacted sample units with sizes of 15 mm diameter by 5 mm thickness were treated by immersing them in a 5% HCl solution for 24 hours with a drying process at 130 ºC for 4 h. After washing and drying, the samples were weighed and the percentages of weight loss were calculated by taking the initial mass (m_o) and final mass (m_f) of each of the materials. It was determined using an analytical balance in triplicate with a measurement error of ± 0.0001 g [12]. No mass loss was obtained after carrying out the previous process to 5 samples, which shows us the durability of the sintered glass-ceramic samples at 1000 and 1050 ºC for 2 hours; this correlates with the volume of the crystalline phases and shows excellent chemical resistance behavior for both samples. The achievement of a high chemical durability in glass-ceramics indicates that the chemical composition of the crystalline phases obtained favors a good stability. Generally, glass-ceramic materials have good chemical stability and often compare favorably with other ceramic-type materials. An increase in the content of the crystalline phase results in greater chemical resistance in glass-ceramic materials [26].

3.5. Density and porosity

Using the ASTM C20-ASTM C373 standards [11,12], we calculated the porosity and density of the glass-ceramic materials obtained by sintering cold compacted powder samples. The data obtained are shown in Table 1, where it was observed that the highest bulk density obtained was 2.57 g/cm^{-3} sintered at 1050 ºC for 2 hours. However, it was evident that the lower the sintering temperature the lower the density value (1.97 g/cm^{-3}), values that are among the range of densities identified for glass-ceramic materials (1.6–3.61 g/cm^{-3}) in accordance with the data reported by similar investigations [19,27–32]. These values are an important factor in determining porosity, assessing durability and strength of materials. However, this allows us to conclude that it is possible to obtain glass-ceramic material with the use of industrial waste as raw material.

Table 1. Calculations of bulk density, water absorption, open porosity and apparent porosity of samples obtained by sintering cold compacted powder samples.

Samples	Bulk density B (g/cm^3)	Water absorption (%)	Open porosity VOP (g/cm^3)	Apparent porosity P (%)
1000 ºC for 2h	1.97	29.21	1.96	39.84
1050 ºC for 2h	2.57	10.79	1.35	27.76

The porosity and water absorption values of samples sintered at 1050 ºC for 2 hours are lower than those sintered at 1000 ºC for 2 hours, an aspect associated with the degree of crystallization of the material due to the heat treatment. The presence of pores in the samples was also confirmed by SEM observations. The factors that regulate the physical, mechanical and chemical properties are the crystalline phase, the degree of crystallization, the size of the crystallites and the homogeneity of the crystal size [17]. The density, water absorption and porosity values of the samples produced indicated that the sample treated at 1050 ºC for 2 hours had the highest degree of crystallization presenting lower porosity, lower percentage of water absorption and higher density compared to the material sintered at 1000 ºC. The fine-grained glass-ceramic materials have better properties, due to

greater cohesion between the particles, which allows for greater mechanical resistance of the material, in which with the increase in the degree of crystallization, the crystallites are strongly interlaced to form a denser crystalline structure and the amorphous glass phase gradually decreases.

3.6. Mechanical properties—compression analysis

The compressive strength of the sintered material at 1000 ºC was 1.78 MPa which increased when the material was sintered at 1050 ºC reaching a value of 8.71 MPa, clearly showing an 80% increase in mechanical strength. One of the factors that influence this aspect is the porosity, in which the mechanical properties decrease with the increase of the porosity according to the generalized mixing rule [28], aspect correlated and demonstrated according to the data presented in Table 1. This feature is also associated with a 2.3% increase in the anorthite phase and a 22% increase in the cordierite phase, and a 13% decrease in the gehlenite phase and a 41% decrease in the Augite phase. In addition to the greater cohesion between particles according to the morphology presented in Figure 3, where changes in the material were observed when they were treated at 1050 ºC in relation to those sintered at 1000 ºC, in general it could be established that ESC, CeV and CaV-based glass-ceramic materials, depending on the crystallization temperature, present increased mechanical resistance [18].

4. Conclusions

The glass-ceramic materials have been prepared by direct sintering of the powdered mixtures of slag, fly ash and glass cullet using the cold powder compaction sintering process. The percentages of apparent porosity and open porosity could be controlled by the sintering parameters, by increasing the temperature in order to decrease these values and improve the mechanical resistance. The bulk density obtained is among the ranges of values reported for glass-ceramic materials. The crystalline phases existing in the sintered material at 1000 and 1050 ºC for 2 hours were anorthite, augite, gehlenite and cordierite. The mechanical resistance of glass-ceramics is originated from multiple parameters: while crystallinity plays a role in the mechanical resistance, the microstructural and substructural parameters are changed at elevated temperatures that ultimately impact in the overall mechanical properties of the material. In our study case, larger mechanical resistance was observed for the sample sintered at 1050 ºC. In general, glass-ceramic materials sintered from slag, fly ash and glass cullet could be used in the application of lightweight building components.

Acknowledgements

The authors would like to thank the Government of Boyacá and Colciencias for financial support under Call 733 (2016) and the professor Aldo R. Boccaccini from the Institute for Biomaterials, Department of Engineering and Materials Science, University Erlangen–Nürenberg, 91058 Erlangen, Germany.

Conflict of interest

All authors declare no conflicts of interest in this paper.

References

1. Holand W, Beall GH (2012) *Glass ceramics Technology*, 2 Eds., New Jersey: John Wiley & Sons.
2. Medina JJA (2008) Analysis of change management in implementation of ERP solutions in some enterprises of Colombia and Mexico. *Sotavento MBA* 11: 54–77.
3. Rawlings RD, Wu JP, Boccaccini AR (2006) Glass-ceramics: their production from wastes—a review. *Journal of Materials Science* 41: 733–761.
4. Dhir RK, de Brito J, Ghataora GS, et al. (2018) Use of Glass Cullet in Ceramics and Other Applications, In: Dhir RK, de Brito J, Lye CQ, *Sustainable Construction Materials*, 1 Ed., Cambridge: Woodhead Publishing, 327–387.
5. Cao J, Lu J, Jiang L, et al. (2016) Sinterability, microstructure and compressive strength of porous glass-ceramics from metallurgical silicon slag and waste glass. *Ceram Int* 42: 10079–10084.
6. Clark TJ, Reed JS (1986) Kinetic processes involved in the sintering and crystallization of glass powders. *J Am Ceram Soc* 69: 837–846.
7. Ji R, Zhang Z, Yan C, et al. (2016) Preparation of novel ceramic tiles with high Al_2O_3 content derived from coal fly ash. *Constr Build Mater* 114: 888–895.
8. Chinnam RK, Francis AA, Will J, et al. (2013) Functional glasses and glass-ceramics derived from iron rich waste and combination of industrial residues. *J Non-Cryst Solids* 365: 63–74.
9. Folguer MV, de Oliveira PN, Alarcon OE (2005) Glass-Ceramics obtained from processed slag and fly ash. *Am Ceram Soc Bull* 84: 9201–9205.
10. Valderrama DMA, Cuaspud JAG, Roether JA, et al. (2019) Development and characterization of glass-ceramics from combinations of slag, fly ash, and glass cullet without adding nucleating agents. *Materials* 12: 2032.
11. ASTM C373-88, Standard Test Method for Water Absorption, Bulk Density, Apparent Porosity, and Apparent Specific Gravity of Fired Whiteware Products. ASTM International, 1999. Available from: https://www.astm.org/DATABASE.CART/HISTORICAL/C373-88R99.htm.
12. ASTM C20-00, Standard Test Methods for Apparent Porosity, Water Absorption, Apparent Specific Gravity, and Bulk Density of Burned Refractory Brick and Shapes by Boiling Water. ASTM International, 2015. Available from: https://www.astm.org/Standards/C20.htm.
13. Ristić MM, Milosević SD (2006) Frenkel's Theory of Sintering. *Sci Sinter* 38: 7–11.
14. Paucar Álvarez CG (2016) Low thermal expansion glass ceramics by sintering and concurrent crystallization of $Li_2O.Al_2O_3.XSiO_2$ glass particles [PhD's thesis]. Autonomous University of Madrid, Madrid.
15. Scherer GW (1986) Viscous sintering under a uniaxial load. *J Am Ceram Soc* 69: 206–207.
16. Moreira ML, Pianaro SA, Cava SS, et al. (2009) Development of glass-ceramic materials of high hardness based on the systems SiO_2–Al_2O_3–CaO y SiO_2–Al_2O_3–Nb_2O_5. *Ceram Inform* 326: 75–80.
17. Erol M, Küçükbayrak S, Ersoy-Meriçboyu A (2007) Production of glass-ceramics obtained from industrial wastes by means of controlled nucleation and crystallization. *Chem Eng J* 132: 335–343.
18. Öveçoğlu ML (1998) Microstructural characterization and physical properties of a slag-based glass-ceramic crystallized at 950 and 1100 ºC. *J Eur Ceram Soc* 18: 161–168.

19. Rawlings RD, Wu JP, Boccaccini AR (2006) Glass-ceramics: their production from wastes—a review. *J Mater Sci* 41: 733–761.
20. Zhao L, Wei W, Bai H, et al. (2015) Synthesis of steel slag ceramics: chemical composition and crystalline phases of raw materials. *Int J Miner Metall Mater* 22: 325–333.
21. Cheng TW (2003) Combined glassification of EAF dust and incinerator fly ash. *Chemosphere* 50: 47–51.
22. Leguey S, Carretero MI, Fabbri B, et al. (2001) Mineralogical and chemical characterization of the bricks at Torre del Oro in Seville: an approximation to the firing temperature and origin of the raw materials. *Bol Soc Esp Ceram V* 40: 457–461.
23. Qin J, Yang C, Cui C, et al. (2016) $Ca2^{+}$ and OH^{-} release of ceramsites containing anorthite and gehlenite prepared from waste lime mud. *J Environ Sci* 47: 91–99.
24. Shyu JJ, Wang CY, Chang TY (1996) Controlled phase transformations by glass particle size in spodumene and cordierite glass-ceramics. *J Am Ceram Soc* 79: 1971–1974.
25. Fernández-Jiménez A, de la Torre AG, Palomo A, et al. (2006) Quantitative determination of phases in the alkaline activation of fly ash. Part II: Degree of reaction. *Fuel* 85: 1960–1969.
26. Oziel M, Alicia V, Mendez AA (2011) Obtaining a glass-ceramic material from a steel slag mixed with glass cullet. *Bol Soc Esp Ceram V* 50: 143–150.
27. Diaz IN, Marchal M, Irùn M, et al. (2000) *New Technologies for the Ceramic Sector*, Castelló de la Plana: Universidad Jaume I.
28. Ureña MLP (2011) In-situ characterization of ash of some Colombian coals by gamma-gamma backscatter [Master's thesis]. Universidad Nacional de Colombia, Colombia.
29. Boccaccini AR, Trusty PA, Taplin DMR (1995) Anisotropic shrinkage of barium-magnesium aluminosilicate glass powder compacts during sintering. *Mater Lett* 24: 199–205.
30. Aloisi M, Karamanov A, Pelino M (2004) Sintered glass–ceramic from municipal solid waste incinerator ashes. *J Non-Cryst Solids* 345: 192–196.
31. Ghosal S, Self SA (1995) Particle size-density relation and cenosphere content of coal fly ash. *Fuel* 74: 522–529.
32. Ji S, Gu Q, Xia B (2006) Porosity dependence of mechanical properties of solid materials. *J Mater Sci* 41: 1757–1768.

AIMS Press